Received: 26 November 2020 | Revised: 5 January 2021 | Accepted: 5 January 2021

DOI: 10.1002/bit.27673

ARTICLE

BIOTECHNOLOGY AND BIOENGINEERING WILEY

A CRISPR-Cas12a-derived biosensor enabling portable personal glucose meter readout for quantitative detection of SARS-CoV-2

Di Huang[1,2] | Zhuwei Shi[1,2] | Jiajie Qian[1,2] | Ke Bi[1,2] | Mengjun Fang[1,2] | Zhinan Xu[1,2]

[1]Key Laboratory of Biomass Chemical Engineering of Ministry of Education, College of Chemical and Biological Engineering, Zhejiang University, Hangzhou, China

[2]Institute of Biological Engineering, College of Chemical and Biological Engineering, Zhejiang University, Hangzhou, China

Correspondence
Zhinan Xu, Institute of Biological Engineering, College of Chemical and Biological Engineering, Zhejiang University, Hangzhou 310027, China.
Email: znxu@zju.edu.cn

Funding information

National Key Research and Development Program of China, Grant/Award Number: 2018YFA0901800, 2018YFC1603902; The Science and Technology Development Project of Hangzhou, Grant/Award Number: 20202013A02; National Natural Science Foundation of China, Grant/Award Numbers: 21576232, 21808199

Abstract

Severe acute respiratory syndrome coronavirus 2 (SARS-CoV-2) has spread rapidly throughout the whole world and caused significant difficulties in the prevention and control of the epidemic. In this case, several detection methods have been established based on nucleic acid diagnostic techniques and immunoassays to achieve sensitive and specific detection of SARS-CoV-2. However, most methods are still largely dependent on professional instruments, highly trained operators, and centralized laboratories. These limitations gravely diminish their practicality and portability. Herein, a clustered regularly interspaced short palindromic repeats (CRISPR) Cas12a based assay was developed for portable, rapid and sensitive of SARS-CoV-2. In this assay, samples were quickly pretreated and amplified by reverse transcription recombinase-aided amplification under mild conditions. Then, by combining the CRISPR Cas12a system and a glucose-producing reaction, the signal of the virus was converted to that of glucose, which can be quantitatively read by a personal glucose meter in a few seconds. Nucleocapsid protein gene was tested as a model target, and the sensitivity for quantitative detection was as low as 10 copies/μl, which basically meet the needs of clinical diagnosis. In addition, with the advantages of lower material cost, shorter detection time, and no requirement for professional instrument in comparison with quantitative reverse transcription-polymerase chain reaction, this assay is expected to provide a powerful technical support for the early diagnosis and intervention during epidemic prevention and control.

KEYWORDS

CRISPR Cas12a, personal glucose meter, point-of-care biosensor, portable detection, SARS-CoV-2

1 | INTRODUCTION

Severe acute respiratory syndrome coronavirus 2 (SARS-CoV-2) is a novel coronavirus, and the disease caused by this virus, termed COVID-19, presented acute respiratory distress syndrome, resulting in a surge of pulmonary, respiratory failure and secondary bacterial infection (Wu et al., 2020; Zhou et al., 2020; Zhu et al., 2020). Compared with other pathogenic viruses, such as SARS, MERS, and HIV, SARS-CoV-2 with a medium mortality rate and reproduction rate was so deceptive that the epidemic situation spread out rapidly

to the whole world (Baud et al., 2020; Sanche et al., 2020; Zhao et al., 2020). Recent research reported that early intervention of COVID-19 would not only reduce the crest value of confirmed cases but also delay the arrival of the crisis (Pokhrel et al., 2020).

On this occasion, early diagnosis is necessary to satisfy the actual needs of effective intervention for curbing the epidemic outbreak (Cui & Zhou, 2020; Ji et al., 2020). However, traditional diagnostic methods, including computed tomography (CT) imageological examinations, immunoassays, and viral RNA-based assays, are facing severe challenges in many aspects, such as sensitivity, specificity, cost, time consumption, and so forth (Feng et al., 2020). To be specific, chest CT scans showed relatively low specificity and only diagnose patients at the later stage after infections. Immunoassays were developed for the detection of immunoglobulin G (IgG) and immunoglobulin M (IgM) in serum samples (Carter et al., 2020; Ou et al., 2020), which showed high sensitivity and selectivity based on antigen-antibody interactions (Garg et al., 2021). Unfortunately, it took approximately 13 days after infection for the seroconversion of IgG and IgM at a detectable level, making early diagnosis nearly impossible. Consequently, more attention was focused on the molecular diagnosis of viral RNA. Since (Wu et al., 2020) the first release of the SARS-CoV-2 genome sequence (GeneBank accession number: MN908947), several viral RNA-based assays have been developed to detect specific genome segments of SARS-CoV-2 (Yan et al., 2020). For example, in a reverse transcription-polymerase chain reaction (RT-PCR), viral RNA was converted into complementary DNA (cDNA) by reverse transcription, followed by PCR amplification (Chu et al., 2020). Quantitative RT-PCR (qRT-PCR) assays were further developed to record the fluorescent signals during the amplification in a real-time manner to quantify the target viral RNA. Taking advantage of high sensitivity (1–10 copies/μl), qRT-PCR has been regarded as the clinical gold standard for SARS-CoV-2 diagnosis and detection (Chan et al., 2020; Xie et al., 2020). However, professional instrument was required, the whole process took skilled operators 4–6 h to obtain the test results, and the turnaround time for clinical samples from patients to laboratories was generally more than 1 day. In other words, early diagnosis and intervention were still challenging and even impractical particularly for developing countries at present stage. Therefore, a point-of-care (POC) testing approach which can achieve fast, sensitive, and specific detection of SARS-CoV-2 by any user at any given time and place in the absence of professional instruments is highly demanded to satisfy the needs of early diagnosis and intervention.

In recent years, clustered regularly interspaced short palindromic repeats (CRISPR) and CRISPR associated (Cas) enzymes have been playing increasingly important roles part in both genome editing and nucleic acid detection (Zhu et al., 2020). For instance, with the mediation of CRISPR RNA (crRNA), Cas12a can recognize specific DNA sequences and exhibit nonspecific single-stranded DNA (ssDNA) cleavage activity (Swarts & Jinek, 2019; Yamano et al., 2016). Based on such trans-cleavage activities, CRISPR Cas12a has been transformed into several biosensors for the detection of nucleic acid targets, such as single-nucleotide polymorphism (Li et al., 2018; Shao et al., 2019), pathogenic bacteria (Chen et al., 2020; Wang et al., 2020), bacterial resistances (English et al., 2019; Xu et al., 2020), and viruses (Chen et al., 2018; Tsou et al., 2019). What's more, several biosensors for sensitive detection of SARS-CoV-2 have been established by combining CRISPR Cas12a with isothermal amplification methods, such as reverse transcription loop-mediated isothermal amplification and recombinase polymerase amplification (RPA). Nevertheless, there is still plenty of room for further improvement of these methods in terms of signal readout. For example, the test strips only provide qualitative results and the fluorescent reporter system still suffers from the requirement of professional instruments and well-trained operators (Broughton et al., 2020; Huang et al., 2020). On the contrary, personal glucose meter (PGM) is one of the most mature and successful examples of POC testing, with advantages of low cost, mini size, portable operation, and reliable quantitative results. Although PGMs were mainly used in blood glucose monitoring, their applications could be expanded by combining with magnetic beads (MBs) and aptamer or antibody-conjugated invertase, which transformed target/aptamer or antigen-antibody recognition signal into invertase release followed by the conversion to glucose signal. In this way, portable PGMs have been developed for POC testing of several nonglucose targets, such as clinical biomarkers (Xiang & Lu, 2011), drugs (Xiang et al., 2014), heavy metal ions (Xiang & Lu, 2013), and toxins (Gu et al., 2015). Therefore, the combination of CRISPR Cas12a, signal transduction, and PGMs should enable the establishment of a portable household biosensor platform for rapid, sensitive, specific, and quantitative detection of SARS-CoV-2.

Herein, we present a CRISPR Cas12a-derived biosensing platform for quantitative POC testing of SARS-CoV-2 using PGMs. In this method, reverse transcription recombinase-aided amplification (RT-RAA) is used to convert target viral RNA into cDNA and achieve exponential amplification under constant and mild temperatures. With the mediation of crRNA, Cas12a specifically recognizes the amplified DNA and exhibits its ssDNA cleavage activity. In this way, ssDNA-conjugated invertase on MBs is released by activated Cas12a, and the signal was further transformed by glucose-producing reaction for final readout by portable PGMs. Using this CRISPR Cas12a-derived biosensor, SARS-CoV-2 can be quantitatively detected by PGMs. With the advantages of high sensitivity, selectivity, portability, and low-cost, the method reported here can be applied in quantitative testing SARS-CoV-2 loads in samples by any users at any given time and place, and provide a useful tool in early diagnosis and intervention during epidemic prevention and control.

2 | MATERIALS AND METHODS

2.1 | Materials

LbaCas12a and NEBuffer 2.1 were the products of New England Biolabs Inc. Streptavidin MBs M-280 were purchased from Thermo

Fisher Scientific. Amicon ultrafiltration tubes were purchased from Millipore Inc. Invertase (*Saccharomyces cerevisiae*), 4-(N-Maleimidomethyl) cyclohexane-1-carboxylic acid 3-sulfo-N-hydroxysuccinimide ester sodium salt (sulfo-SMCC), and tris (2-carboxyethyl) phosphine (TCEP) were obtained from Sigma-Aldrich, Inc. Oligonucleotides used in this article (Table S1) and SARS-CoV-2 pseudovirus were purchased from TsingKe Biological Technology. RNase inhibitor and portable magnetic separation devices were bought from Sangon Biotech. All other chemicals were of analytical grade and were purchased from Sinopharm Chemical Reagent Co., Ltd. The PGM was purchased from Roche Diagnostics Co., Ltd. SARS-CoV-2 samples were obtained from Biocome Inc., and other virus samples were obtained from the Children's Hospital of Zhejiang University School of Medicine.

2.2 | Viral RNA extraction and sample pretreatment assay

SARS-CoV-2 pseudovirus genome containing N, M, E, and S genes was extracted by extraction and purification kits (Tiangen Biotech Co., Ltd.) to investigate the feasibility and sensitivity of CRISPR assay. All real samples (nasopharyngeal or oropharyngeal swabs) were heat-treated in CDC or hospitals (60°C, 30 min) to preinactivate the viruses. The virus samples were further treated by commercial lysis and RNA protective buffer (Biolab Co., Ltd.) for CRISPR assay (extraction-free, about 10 min), or extracted by extraction and purification kits according to the procedure of CDC assays (about 30 min) for qRT-PCR assay.

2.3 | In vitro preparation of nucleic acids

The double stranded DNAs (dsDNAs) mimicking the fragments of different SARS-CoV-2 genes were prepared through annealing of two synthesized ssDNA (shown in Table S1) and stored at −20°C for further use. For crRNA preparation, in vitro transcription was carried out through incubating the reaction system containing 6 μl 5 μM dsDNA template with a T7 promoter, 8 μl NTP mixtures (10 mM each), 2 μl TranscriptAid enzyme mixtures, and 4 μl buffer from kits (Thermo Fisher Scientific) at 37°C for 8 h. Then the transcription products were treated by DNaseI to digest the DNA, and the crRNA was further purified using RNA clean and concentrator kits (Zymo Research). After quantification using a UV-vis spectrophotometer, the crRNA was stored at −80°C for further use.

2.4 | RT-RAA assay for genome fragments of SARS-CoV-2

Primers for RT-RPA reactions were designed with Primer-BLAST in NCBI. According to the instructions of RT-RAA kits (ZhongCe Bio-Technology Co., Ltd.), enzyme mixtures were dissolved by 41.5 μl buffer A and mixed with 4 μl 5 μM Primers (shown in Table S1), 2 μl pretreated samples, and 2.5 μl buffer B in order. After incubation at 42°C for 20 min, the products were used for CRISPR assay directly.

2.5 | Fluorescence-CRISPR assay

The fluorescence-CRISPR assay was composed of 50 nM Cas12a, 100 nM crRNA, 750 nM fluorescence substrates, 10 U of RNase inhibitor, 1 μl dsDNA target, and 1× NEBuffer 2.1 (10 mM Tris-HCl, 50 mM NaCl, 10 mM $MgCl_2$, 100 μg/ml BSA, 1 mM DTT, pH 7.9). This 20 μl assembled mixture was transferred to 384-well plates for incubating at 37°C with fluorescence measurements taken every 3 min by a Thermo Scientific Varioskan Flash Multimode Plate Reader (λ_{Ex}: 535 nm, λ_{Em}: 556 nm).

2.6 | Preparation of invertase-modified MBs

Invertase-modified MBs were synthesized by chemical coupling following the previously established procedures (Tian et al., 2017; Xiang & Lu, 2011). A total of 1 μl 30 mM TCEP and 1 μl 1 M sodium phosphate buffer (pH 5.5) were added to every 15 μl 1 mM thiol-DNA-biotin in ddH_2O and mixed at room temperature for thiol activation. After incubation for 1 h, the mixture was then purified by ultrafiltration (Amicon-3K) using washing buffer (0.1 M NaCl, 0.1 M sodium phosphate buffer, pH 7.3) for six times. For invertase conjugation, 1 mg sulfo-SMCC was added to 400 μl 20 mg/ml invertase in ddH_2O, and the mixture was rotated at room temperature for 1 h. After centrifugation to remove extra sulfo-SMCC, the solution was further purified by ultrafiltration (Amicon-100K) using washing buffer for six times. Subsequently, the purified thiol-DNA-biotin and sulfo-SMCC-activated invertase were mixed and kept at room temperature on a rotator for 48 h. To remove unconjugated thiol-DNA-biotin, the mixture was purified by ultrafiltration (Amicon-100K) using washing buffer for six times. To prepare invertase-modified MBs, every 1 nmol conjugate obtained from the above method was mixed with 10 μl 10 mg/ml streptavidin MBs at room temperature for 15 min, followed by purification by a magnet using PBS buffer with 0.05% Tween-20 for six times. Finally, invertase-modified MBs were resuspended in 50 μl preservation solution (0.1 M NaCl, 0.1 M sodium phosphate buffer, 0.05% Tween-20, pH 7.3) and stored at 4°C for further use.

2.7 | PGMs-CRISPR assay

In a typical PGMs-CRISPR assay, after removing the preservation solution, 10 μl MBs were mixed with 50 nM Cas12a, 100 nM crRNA, 15 U of RNase inhibitor, 1 μl dsDNA target or RT-RAA products, and 1× NEBuffer 2.1 with a final volume of 30 μl. After reaction at 37°C for 30 min, 20 μl supernate was separated by a magnet and mixed with 30 μl 1 M sucrose, 6 μl reaction buffer (0.1 M sodium citrate buffer, pH 5.6), and 4 μl ddH_2O. After incubation at 37°C for 30 min, 2 μl of the solution was removed for signal readout by a commercial PGM in seconds.

2.8 | One-step qRT-PCR assay

One-step qRT-PCR assay was conducted in the StepOnePlus Real-Time PCR Systems. According to the instruction manual of the qRT-PCR kit (BioGerm Co., Ltd.), 25 μl one-step qRT-PCR assay contained 5 μl pretreated samples, 4 μl enzyme mixtures, 4 μl primers and fluorescence probes, and 12 μl qRT-PCR buffer. The thermal cycling protocol included 10 min at 50°C for RNA reverse transcription, 5 min at 95°C for DNA preactivation, 40 cycles of amplification (10 s at 95°C for denaturation, 40 s at 55°C for annealing, extension, and signal readout). 6-Carboxy-fluorescein (FAM) and 5-hexachloro-fluorescein (HEX) signal respectively represented the detection results of N gene and ORF1ab of SARS-CoV-2, and the fluorescence thresholds were set as ten times the standard deviation in cycle 3–15.

3 | RESULTS

3.1 | Working principle of SARS-CoV-2 detection based on PGMs-CRISPR assay

As illustrated in Figure 1, the PGMs-CRISPR assay for SARS-CoV-2 detection mainly includes four parts, pretreatment and isothermal amplification, CRISPR Cas12a system with invertase-modified MBs, glucose-producing reaction, and results readout based on a PGM. Specifically, SARS-CoV-2 in the swab samples was firstly treated by a convenient lysis kit, and the viral contents were released into the solution. The viral RNA in the lysate was further amplified by RT-RAA, generating complementary dsDNA with specific sites for detection. Mediated by crRNA, the dsDNA target can trigger the single-stranded DNase activity of Cas12a, resulting in the cleavage of the ssDNA linker strand between invertase and MBs. Therefore, a quantity of invertase was released from residual MBs by magnetic separation and catalyzed the conversion of sucrose to glucose. With the help of a PGM, the results can be expediently read by any untrained users in seconds. Since the concentration of glucose is positively correlated with that of the virus, it can be regarded as the basis of quantitative detection. In general, this assay can be carried out under mild conditions, and no professional instruments or trained operators were required for the whole detection procedures. Consequently, the assay was expected to provide a useful and portable tool for early diagnosis of SARS-CoV-2.

3.2 | Selection of detection sites on the genome of SARS-CoV-2

Figure 2a showed the genome organization of SARS-CoV-2 and the relative positions of different genes detected by existing nucleic acid testing methods (ORF: open reading frame; S: spike protein; E:envelope protein; M: membrane protein; N: nucleocapsid protein). To find a suitable detection site on the viral genome, the sequence of SARS-CoV-2 (GenBank: NC_045512) was compared with two other SARS-like coronaviruses, bat SARS-like coronavirus (GenBank: MG772933) and SARS-CoV (GenBank: NC_004718). As shown in Figure S1, two specific loci for each gene in SARS-CoV-2 with protospacer adjacent motif (termed N_1, N_2, M_1, M_2, E_1, E_2, S_1, and S_2), which were significantly different in other two viral genomes, were selected to establish the detection system based on CRISPR Cas12. Then the performance of the fluorescence-CRISPR assay was investigated with or without the addition of 10 nM dsDNAs, which were chemically synthesized and had the same sequences as the SARS-CoV-2 gene fragment. The fluorescence intensity of each group was measured every 3 min. As shown in Figure 2b, the reaction kinetics represented the difference in detection sensitivity (Figure 2c). Since N_1 fragment showed a relatively fast reaction rate among eight groups, it was selected as the detection site on the viral genome in the following study.

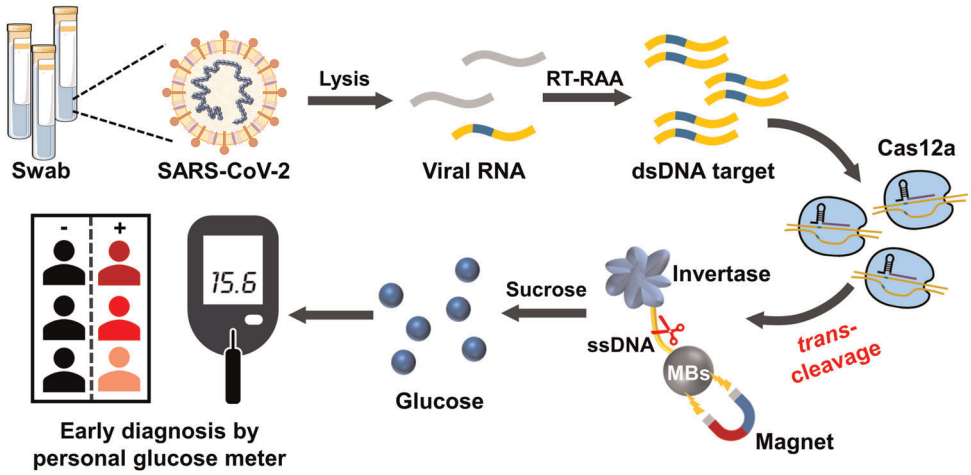

FIGURE 1 Working principle of CRISPR Cas12a-derived biosensor enabling portable personal glucose meter readout for quantitative detection of SARS-CoV-2. CRISPR, clustered regularly interspaced short palindromic repeats; SARS-CoV-2, severe acute respiratory syndrome coronavirus 2 [Color figure can be viewed at wileyonlinelibrary.com]

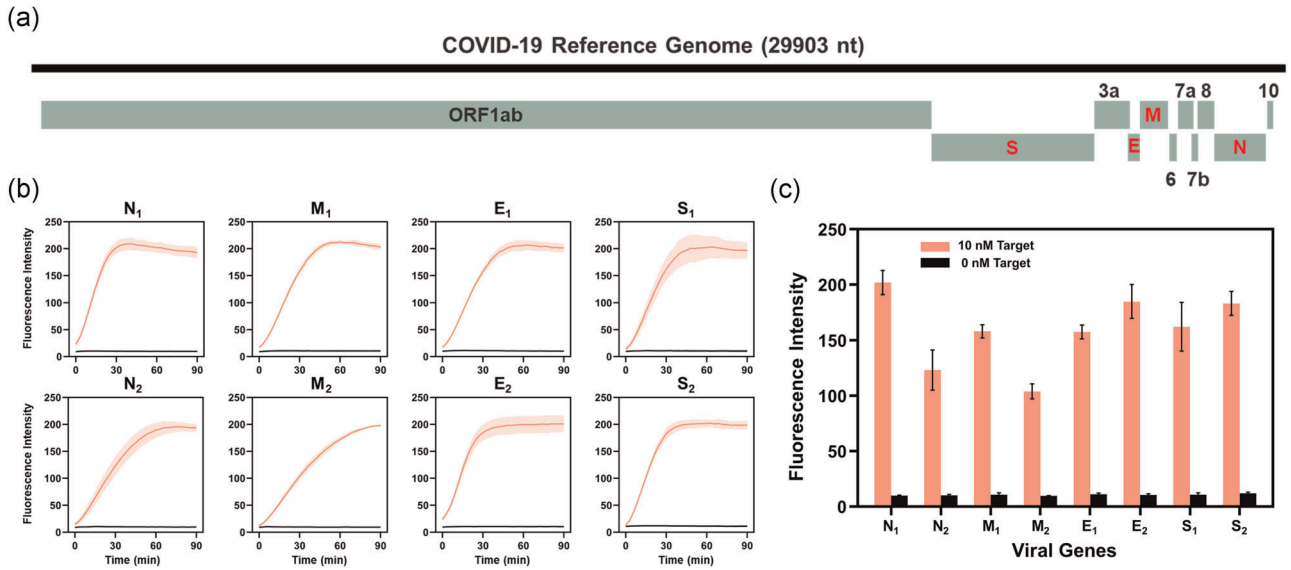

FIGURE 2 Selection of detection sites on the genome of SARS-CoV-2. (a) Genome organization of SARS-CoV-2 and the relative positions of different genes detected by existing nucleic acid testing methods (shown in red). (b) Reaction kinetics of N_1, N_2, M_1, M_2, E_1, E_2, S_1, and S_2 in the fluorescence-CRISPR assay system. The fluorescence intensity was measured every 3 min using a 384-well microplate reader (the mean of three measurements was shown in the curves, and the error bar was shown as the shade). (c) Comparison of the fluorescence intensity of N_1, N_2, M_1, M_2, E_1, E_2, S_1, and S_2 in the fluorescence-CRISPR assay at 30 min (with three biological replicates; error bars represent the mean ± *SD*). CRISPR, clustered regularly interspaced short palindromic repeats; SARS-CoV-2, severe acute respiratory syndrome coronavirus 2 [Color figure can be viewed at wileyonlinelibrary.com]

3.3 | Sensitivity of SARS-CoV-2 detection system based on fluorescence-CRISPR assay

To evaluate the detection sensitivity of N_1 on the genome of SARS-CoV-2, 2 μl extractive samples from different copy numbers of SARS-CoV-2 pseudovirus (0, 1, 5, 10, 10^2, 10^3, and 10^4 copies/μl) were amplified by RT-RAA and analyzed by the fluorescence-CRISPR assay. The fluorescence intensity of each group was measured every 3 min to determine the reaction kinetics (Figure 3a). The group with 1 copy/μl genome of pseudovirus still showed a significant difference in fluorescence intensity with the blank group (*$p < .05$; Figure 3b), indicating that the fluorescence-CRISPR assay demonstrated an excellent sensitivity to detect the target gene on the genome of SARS-CoV-2 pseudovirus and was expected to perform well in actual testing.

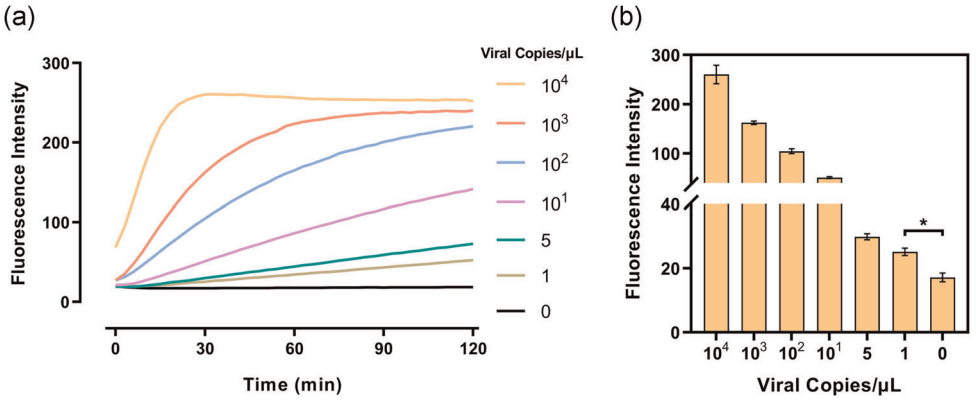

FIGURE 3 Sensitivity of N_1 in the fluorescence-CRISPR assay. (a) Reaction kinetics of N_1 with different pseudovirus genome doages in the fluorescence-CRISPR assay. The serially diluted pseudovirus genome was employed as the detection target, and the fluorescence intensity was measured every 3 min (the mean of three measurements was shown in the curves). (b) Sensitivity of the fluorescence-CRISPR assay at 30 min. The results indicated that the limit of detection could be as low as 1 copy/μl (with three biological replicates; error bars represent the mean ± *SD*; *$p < .05$ in "Student's *t* test"). CRISPR, clustered regularly interspaced short palindromic repeats; SARS-CoV-2, severe acute respiratory syndrome coronavirus 2 [Color figure can be viewed at wileyonlinelibrary.com]

3.4 | Feasibility of SARS-CoV-2 detection system based on PGMs-CRISPR assay

To establish the PGMs-CRISPR assay, the sensitivity of glucose-producing reaction using invertase was first confirmed by PGMs. As shown in Figure S2, the dynamic range of glucose tested by Roche PGMs was 0.6–33.3 mM, and the corresponding concentration of invertase was 0.05–2 μg/ml. What's more, because there was a positive correlation between the concentration of glucose with that of invertase in 0.05–1 μg/ml, a quantitative detection assay was expected to be established in this range. Subsequently, the chemical coupling of invertase and ssDNA was prepared and characterized by sodium dodecyl sulfate polyacrylamide gel electrophoresis (Figure S3), and an extra band with larger molecular weight represented the conjugate. After the preparation of invertase-modified MBs, Cas12a activated by the related target and DNaseI, which possessed a similar nonspecific, single-stranded DNase activity, were respectively involved to verify the feasibility of PGMs-CRISPR assay. As shown in Figure S4, with the presence of 90.9 U/ml DNaseI or 50 nM Cas12a activated by different concentrations of dsDNA, ssDNA linkers were cleaved to release sufficient amount of invertase from the surface of modified MBs, leading to an increase in the concentration of glucose. Note that there was a significant difference in the glucose signal whether 1 nM target dsDNA were supplemented or not (**$p < .01$), which further indicated the feasibility of SARS-CoV-2 detection based on PGMs-CRISPR assay.

3.5 | Performance of PGMs-CRISPR assay in SARS-CoV-2 pseudovirus detection

The genomes of SARS-CoV-2 pseudovirus were tested to further verify the potential clinical application of PGMs-CRISPR assay. A series of concentrations of pseudovirus genomes from 0 to 10^4 copies/μl were amplified by RT-RAA and measured by established PGMs-CRISPR assay as described above. As shown in Figure 4a, different concentrations of pseudovirus genomes resulted in different glucose signals by the glucose-producing reaction, and a significant difference in glucose signals between 10 copies/μl group and the blank group was observed by PGMs (*$p < .05$). In addition, a linear relation between the "Δ concentration of glucose", representing the glucose signals relative to that of the blank sample, and $\log_{10}$ ("the concentrations of pseudovirus genomes") was exhibited in Figure 4b, and the standard curve showed an excellent fit ($R^2 = .994$) within a dynamic range of 10–10^4 copies/μl. Hence, using the formula: $Y = 7.040 \times \log_{10}(X) - 4.785$ (Y: concentration of glucose (mM); X: concentration of pseudovirus genomes (copies/μl)), quantitative detection of pseudovirus genomes was achieved within the dynamic range, indicating a good performance of PGMs-CRISPR assay in the detection of viral genomes. What's more, another detection system based on PGMs-CRISPR assay was established using the same protocol to detect human RNaseP as a reference gene to monitor the reliability of the samples, ensure detection accuracy and avoid false negatives in clinical testing. As to this system, the glucose signal generated by 10^2 copies/μl human RNaseP gene showed a significant difference with that of blank (Figure 4c). Based on the established detection systems targeting N_1 gene and human RNaseP, this PGMs-CRISPR assay is expected to be applied for clinical testing of SARS-CoV-2.

3.6 | Detection of SARS-CoV-2 in clinical samples using PGMs-CRISPR assay

After demonstrating the feasibility of detecting SARS-CoV-2 pseudovirus genome using PGMs-CRISPR assay, clinical samples from

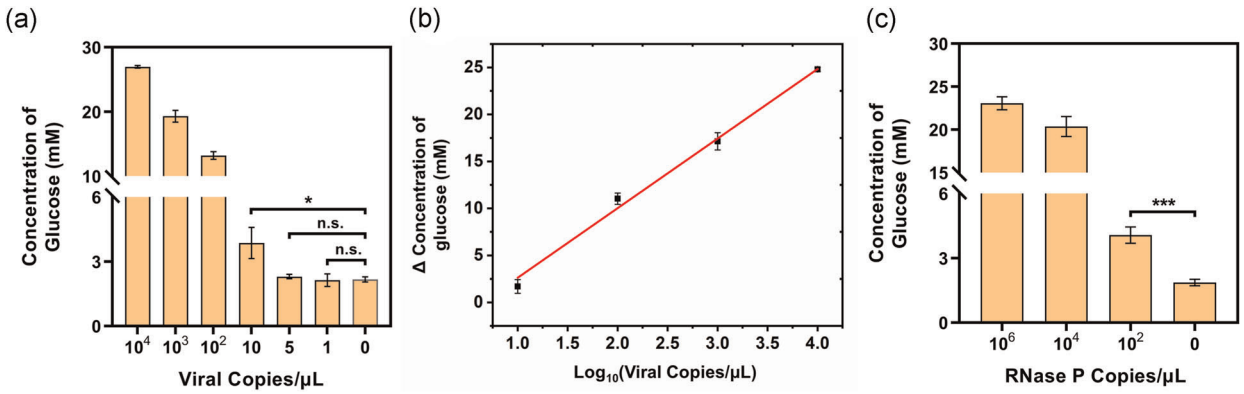

FIGURE 4 Performance of PGMs-CRISPR assay in SARS-CoV-2 pseudovirus detection. (a) Relationship between the concentration of glucose and serially diluted pseudovirus genome after 30 min for Cas12a-cleavage and another 30 min for glucose-producing reaction (with three biological replicates; error bars represent the mean ± *SD*; *$p < .05$, and "n.s." means no significance in "Student's *t* test"). (b) Linear response of the concentration of glucose versus $\log_{10}$ (the concentrations of pseudovirus genomes; with three biological replicates; error bars represent the mean ± *SD*; $R^2 = .994$). (c) Relationship between the concentration of glucose and serially diluted RNaseP gene after 30 min for Cas12a-cleavage and another 30 min for glucose-producing reaction (with three biological replicates; error bars represent the mean ± *SD*; ***$p < .001$ in "Student's *t* test"). CRISPR, clustered regularly interspaced short palindromic repeats; PGM, personal glucose meter; SARS-CoV-2, severe acute respiratory syndrome coronavirus 2 [Color figure can be viewed at wileyonlinelibrary.com]

two patients with SARS-CoV-2 infection, two healthy volunteers without SARS-CoV-2 infection, five patients infected with other four seasonal viruses (Influenza A virus, FluA; Coxsackievirus-A16, Cox-A16; Enterovirus-71, EV-71; Enteric cytopathic human orphan virus-11, Echo-11), and two throat swab samples from healthy volunteers spiked with 200 copies/μl N gene fragments of bat SARS-like coronavirus or SARS-CoV were simply pretreated and analyzed using this established PGMs-CRISPR assay. Glucose signal intensities from PGMs were normalized to the highest value within the N gene or RNaseP set. The final determination for SARS-CoV-2 detection results was according to Figure 5a, with results indicated in the heat map (Figure 5b). Only clinical samples from two patients with SARS-CoV-2 infection produced obvious glucose signal in both N gene or RNaseP detection system, which could be determined as positive cases. Moreover, no telltale signals of the N gene set were generated by other samples, including the volunteers' samples or any other viral samples, all of which exhibited positive signals in the RNaseP set. All the results above-mentioned suggested that the PGMs-CRISPR assay possessed good specificity and promising potential in clinical detection of SARS-CoV-2.

3.7 | Comparison with qRT-PCR assay in accuracy

To verify the testing accuracy of the PGMs-CRISPR assay, clinical samples from two patients with SARS-CoV-2 infection were further detected by qRT-PCR, the "gold standard" of practical detection of SARS-CoV-2 in health facilities, such as the centralized laboratories of hospitals or centers for disease control and prevention. Specific primers and TaqMan probes in the commercial kits were designed based on the ORF1ab gene and N gene of SARS-CoV-2, and multiple quantitative detections were achieved by professional qPCR instrument using different fluorescence signals. Specifically, two clinical positive samples already tested by the PGMs-CRISPR assay, and extractive samples from different copy numbers of SARS-CoV-2 pseudovirus (0, 5, 50, 250, 10^3, 10^4, and 10^5 copies/μl) were respectively detected by one-step qRT-PCR assay. The linear relation between the Ct values of qRT-PCR systems in both FAM and HEX channels and log10 (the concentrations of pseudovirus genome) is shown in Figure S5. The standard curves were respectively fitted as "$Y = -4.655 \times \log_{10}(X) + 40.920$" and "$Y = -4.585 \times \log_{10}(X) + 41.010$" (Y: Ct value; X: concentration of pseudovirus genomes [copies/μl]) with R^2 values of 0.994 and 0.995. Calculated by the formulas, the quantitative detection results with three biological replicates of pseudovirus genomes (copies/μl) from the PGMs-CRISPR assay and two systems in qRT-PCR are shown in Table 1, indicating a good agreement between the two assays. Besides, more relevant detection parameters were compared in Table S2 between PGMs-CRISPR assay and qRT-PCR. On the basis of an acceptable sensitivity, PGMs-CRISPR assay possessed several advantages, including milder experimental temperature, lower material cost, shorter detection time, and no requirement for professional instruments.

TABLE 1 Quantitative detection results from different assays

Detection methods	SARS-CoV-2 (1)[a] (copies/μl)	SARS-CoV-2 (2)[a] (copies/μl)
PGMs-CRISPR assay	13.57 ± 0.42	25.85 ± 5.03
qRT-PCR (FAM)	16.88 ± 1.60	28.89 ± 1.17
qRT-PCR (HEX)	15.26 ± 0.07	27.19 ± 1.37

Abbreviation: SARS-CoV-2, severe acute respiratory syndrome coronavirus 2.

[a]$n = 3$, mean ± *SD*. SARS-CoV-2 (1) and (2): two positive samples mentioned in Figure 5.

3.8 | Comparison with other existing assays for SARS-CoV-2 detection

At present, in addition to qRT-PCR and other nucleic acid testing methods, most existing assays for SARS-CoV-2 detection were based on immunoassay, and the detection targets mainly included viral antigen and antigen-specific antibody (Feng et al., 2020). However, the selectivity of antigen-based tests was not good enough to distinguish similar virus, such as SARS-CoV and SARS-CoV-2, and antibody-based tests suffered from a longer window period which

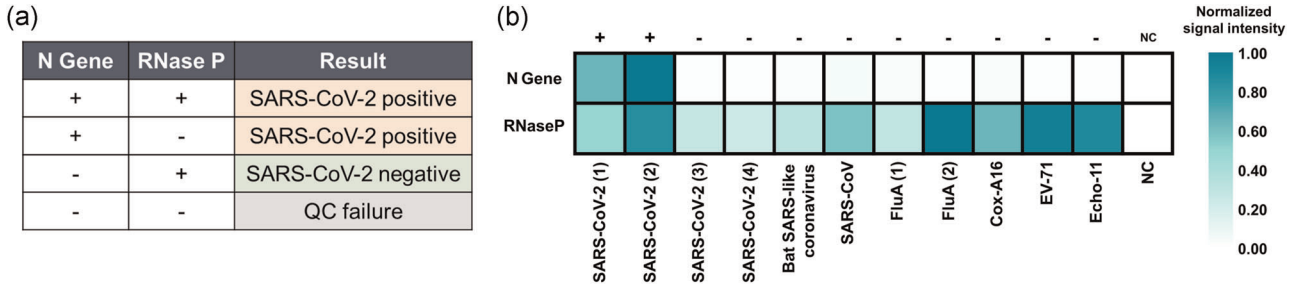

FIGURE 5 Detection of SARS-CoV-2 in clinical samples using PGMs-CRISPR assay. (a) Clinical diagnostic criteria of SARS-CoV-2 according to N_1 gene and RNaseP (QC represents quality control). (b) Heatmap represents normalized mean glucose values of N_1 gene and RNaseP detected in clinical or spiked samples by PGMs-CRISPR assay. CRISPR, clustered regularly interspaced short palindromic repeats; PGM, personal glucose meter; SARS-CoV-2, severe acute respiratory syndrome coronavirus 2 [Color figure can be viewed at wileyonlinelibrary.com]

went against the need of early diagnosis (Ravi et al., 2020). What's more, in terms of dealing with the mutations of SARS-CoV-2, the time and money consumed in antigen or antibody development and synthesis were much more than that in PGMs-CRISPR assay (only sequencing and crRNA adjustment were needed). As shown in Table S3, this PGMs-CRISPR assay exhibited a certain advantage in both materials and instruments price to demonstrate the feasibility of our assay as a POC device. Last but no least, the sensitivity of the assay is also expected to be further improved by means of advanced glucose sensors (Brown et al., 2018. Under this circumstance, the PGMs-CRISPR assay was expected to provide reasonable technical support for the early diagnosis and intervention during epidemic prevention and control, particularly for household test in rural areas.

4 | CONCLUSION

In conclusion, a portable nucleic acid-testing platform based on the CRISPR Cas12a system and a glucose-producing reaction was developed for early diagnosis of SARS-CoV-2. The assay integrated RT-RAA for amplification of the virus genes, CRISPR Cas12a for target recognition, a glucose-producing response for signal transduction, and a PGM for final results readout. Since the advantages of RT-RAA for sensitive amplification at a mild temperature, large and professional instruments were not required in the process. Subsequently, the CRISPR Cas12a system can specifically recognize the target sequences and convert the concentration signal of the target to that of glucose, with the help of invertase-modified MBs and the glucose-producing reaction. Finally, the detection results were read by a portable glucose meter widely used in daily household health monitoring. In this way, the portability and practicability of the SARS-CoV-2 detection system was effectively improved. The established PGMs-CRISPR assay achieved sensitive, specific, and quantitative detection of N gene in SARS-CoV-2 pseudovirus genome within the range of 10–10^4 copies/μl, which was acceptable for early diagnosis. In comparison with qRT-PCR, the clinical golden standard of SARS-CoV-2 detection, the PGMs-CRISPR assay possessed advantages like lower material cost, shorter detection time, milder experimental conditions, and no requirement for professional instrument. Although there are some challenges evident in the development pipeline before actual clinical application, such as reagent storage conditions and multiple reaction steps, the development of modern biotechnologies and analytical tools, such as freeze-drying technology and microfluidic devices, will effectively improve the usability of this assay in practice. There, PGMs-CRISPR assay is expected to provide a portable and effective tool for early diagnosis of SARS-CoV-2 during epidemic prevention and control.

ACKNOWLEDGMENTS

The authors thank the National Key Research and Development Program of China (2018YFC1603902 & 2018YFA0901800), the Science and Technology Development Project of Hangzhou (20202013A02) and the National Natural Science Foundation of China (21576232 & 21808199) for financial support. And we acknowledge Prof. Jiazhang Lian (College of Chemical and Biological Engineering, Zhejiang University) for his careful editing.

CONFLICT OF INTERESTS

The authors declare that there are no conflict of interests.

AUTHOR CONTRIBUTIONS

Di Huang: Formal analysis, Methodology, Writing—original draft. Zhuwei Shi: Investigation, Formal analysis, Validation. Jiajie Qian: Formal analysis, Methodology. Ke Bi: Resources, Validation. Mengjun Fang: Investigation, Validation. Zhinan Xu: Supervision, Project administration, Funding acquisition, Writing—review and editing.

ORCID

Zhinan Xu http://orcid.org/0000-0001-7833-026X

REFERENCES

Baud, D., Qi, X., Nielsen-Saines, K., Musso, D., Pomar, L., & Favre, G. (2020). Real estimates of mortality following COVID-19 infection. *The Lancet Infectious Diseases*, *20*(7), 773. https://doi.org/10.1016/s1473-3099(20)30195-x

Broughton, J. P., Deng, X., Yu, G., Fasching, C. L., Servellita, V., Singh, J., Miao, X., Streithorst, J. A., Granados, A., Sotomayor-Gonzalez, A., Zorn, K., Gopez, A., Hsu, E., Gu, W., Miller, S., Pan, C. Y., Guevara, H., Wadford, D. A., Chen, J. S., & Chiu, C. Y. (2020). CRISPR-Cas12-based detection of SARS-CoV-2. *Nature Biotechnology*, *38*(7), 870–874. https://doi.org/10.1038/s41587-020-0513-4

Brown, S., Zambrana, P. N., Ge, X., Bagdure, D, Stinchcomb, A. L., Rao, G., & Tolosa, L. (2018). Minimally invasive technique for measuring transdermal glucose with a fluorescent biosensor. *Analytical and Bioanalytical Chemistry*, *410*, 7249–7260. https://doi.org/10.1007/s00216-018-1336-8

Carter, L. J., Garner, L. V., Smoot, J. W., Li, Y., Zhou, Q., Saveson, C. J., Sasso, J. M., Gregg, A. C., Soares, D. J., Beskid, T. R., Jervey, S. R., & Liu, C. (2020). Assay techniques and test development for COVID-19 diagnosis. *ACS Central Science*, *6*(5), 591–605. https://doi.org/10.1021/acscentsci.0c00501

Chan, J. F. W., Yip, C. C. Y., To, K. K. W., Tang, T. H. C., Wong, S. C. Y., Leung, K. H., Fung, Ng, A. C., Zou, Z., Tsoi, H. W., Choi, G. K., Tam, A. R., Cheng, V. C., Chan, K. H., Tsang, O. T., Yuen, K. Y., & A. Y. F. (2020). Improved molecular diagnosis of COVID-19 by the novel, highly sensitive and specific COVID-19-RdRp/Hel real-time reverse transcription-PCR assay validated in vitro and with clinical specimens. *Journal of Clinical Microbiology*, *58*(5), 310–320. https://doi.org/10.1128/jcm

Chen, J., Jiang, F., Huang, C. W., & Lin, L. (2020). Rapid genotypic antibiotic susceptibility test using CRISPR-Cas12a for urinary tract infection. *Analyst*, *145*(15), 5226–5231. https://doi.org/10.1039/d0an00947d

Chen, J. S., Ma, E., Harrington, L. B., Costa, M. D., Tian, X., Palefsky, J. M., & Doudna, J. A. (2018). CRISPR-Cas12a target binding unleashes indiscriminate single-stranded DNase activity. *Science*, *360*, 436–439. https://doi.org/10.1126/science.aar6245

Chu, D. K. W., Pan, Y., Cheng, S. M. S., Hui, K. P. Y., Krishnan, P., Liu, Y., Ng, D. Y. M., Wan, C. K. C., Yang, P., Wang, Q., Peiris, M., & Poon, L. L. M. (2020). Molecular diagnosis of a novel coronavirus (2019-nCoV) causing an outbreak of pneumonia. *Clinical Chemistry*, *66*(4), 549–555. https://doi.org/10.1093/clinchem/hvaa029

Cui, F., & Zhou, H. S. (2020). Diagnostic methods and potential portable biosensors for coronavirus disease 2019. *Biosensors and Bioelectronics*, *165*, 112349. https://doi.org/10.1016/j.bios.2020.112349

English, M. A., Soenksen, L. R., Gayet, R. V., de Puig, H., Angenent-Mari, N. M., Mao, A. S., Nguyen, P. Q., & Collins, J. J. (2019). Programmable CRISPR-responsive smart materials. *Science*, *365*(6455), 780–785. https://doi.org/10.1126/science.aaw5122

Feng, W., Newbigging, A. M., Le, C., Pang, B., Peng, H., Cao, Y., Wu, J., Abbas, G., Song, J., Wang, D. B., Cui, M., Tao, J., Tyrrell, D. L., Zhang, X. E., Zhang, H., & Le, X. C. (2020). Molecular diagnosis of COVID-19: Challenges and research needs. *Analytical Chemistry*, *92*(15), 10196–10209. https://doi.org/10.1021/acs.analchem.0c02060

Garg, M., Sharma, A. L., & Singh, S. (2021). Advancement in biosensors for inflammatory biomarkers of SARS-CoV-2 during 2019–2020. *Biosensors and Bioelectronics*, *171*, 112703. https://doi.org/10.1016/j.bios.2020.112703

Gu, C., Lan, T., Shi, H., & Lu, Y. (2015). Portable detection of melamine in milk using a personal glucose meter based on an in vitro selected structure-switching aptamer. *Analytical Chemistry*, *87*(15), 7676–7682. https://doi.org/10.1021/acs.analchem.5b01085

Huang, Z., Tian, D., Liu, Y., Lin, Z., Lyon, C. J., Lai, W., Fusco, D., Drouin, A., Yin, X., Hu, T., & Ning, B. (2020). Ultra-sensitive and high-throughput CRISPR-p owered COVID-19 diagnosis. *Biosensors and Bioelectronics*, *164*, 112316. https://doi.org/10.1016/j.bios.2020.112316

Ji, T., Liu, Z., Wang, G., Guo, X., Akbar Khan, S., Lai, C., Chen, H., Huang, S., Xia, S., Chen, B., Jia, H., Chen, Y., & Zhou, Q. (2020). Detection of COVID-19: A review of the current literature and future perspectives. *Biosensors and Bioelectronics*, *166*, 112455. https://doi.org/10.1016/j.bios.2020.112455

Li, S. Y., Cheng, Q. X., Wang, J. M., Li, X. Y., Zhang, Z. L., Gao, S., Cao, R. B., Zhao, G. P., & Wang, J. (2018). CRISPR-Cas12a-assisted nucleic acid detection. *Cell Discovery*, *4*, 20. https://doi.org/10.1038/s41421-018-0028-z

Ou, X., Liu, Y., Lei, X., Li, P., Mi, D., Ren, L., Guo, L., Guo, R., Chen, T., Hu, J., Xiang, Z., Mu, Z., Chen, X., Chen, J., Hu, K., Jin, Q., Wang, J., & Qian, Z. (2020). Characterization of spike glycoprotein of SARS-CoV-2 on virus entry and its immune cross-reactivity with SARS-CoV. *Nature Communications*, *11*(1), 1620. https://doi.org/10.1038/s41467-020-15562-9

Pokhrel, P., Hu, C., & Mao, H. (2020). Detecting the coronavirus (COVID-19). *ACS Sensors*, *5*(8), 2283–2296. https://doi.org/10.1021/acssensors.0c01153

Ravi, N., Cortade, D. L., Ng, E., & Wang, S. X. (2020). Diagnostics for SARS-CoV-2 detection: A comprehensive review of the FDA-EUA COVID-19 testing landscape. *Biosensors and Bioelectronics*, *165*, 112454. https://doi.org/10.1016/j.bios.2020.112454

Sanche, S., Lin, Y. T., Xu, C., Romero-Severson, E., Hengartner, N., & Ke, R. (2020). High contagiousness and rapid spread of severe acute respiratory syndrome coronavirus 2. *Emerging Infectious Diseases*, *26*(7), 1470–1477. https://doi.org/10.3201/eid2607.200282

Shao, N., Han, X., Song, Y., Zhang, P., & Qin, L. (2019). CRISPR-Cas12a coupled with platinum nanoreporter for visual quantification of SNVs on a volumetric bar-chart chip. *Analytical Chemistry*, *91*(19), 12384–12391. https://doi.org/10.1021/acs.analchem.9b02925

Swarts, D. C., & Jinek, M. (2019). Mechanistic Insights into the cis- and trans-acting DNase activities of Cas12a. *Molecular Cell*, *73*(3), 589–600. https://doi.org/10.1016/j.molcel.2018.11.021

Tian, T., An, Y., Wu, Y., Song, Y., Zhu, Z., & Yang, C. (2017). Integrated distance-based origami paper analytical device for one-step visualized analysis. *ACS Appl. Mater Inter.* *9*(36), 30480–30487. https://doi.org/10.1021/acsami.7b09717

Tiangco, C., Fon, D., Sardesai, N., Kostov, Y., Sevilla, F., Rao, G., & Tolosa, L. (2017). Fiber optic biosensor for transdermal glucose based on the glucosebinding protein. *Sensors and Actuators B: Chemical*, *242*, 569–576. http://dx.doi.org/10.1016/j.snb.2016.11.077.

Tsou, J. H., Leng, Q., & Jiang, F. (2019). A CRISPR test for detection of circulating nuclei acids. *Translational Oncology*, *12*(12), 1566–1573. https://doi.org/10.1016/j.tranon.2019.08.011

Wang, Y., Ke, Y., Liu, W., Sun, Y., & Ding, X. (2020). A one-pot toolbox based on Cas12a/crRNA enables rapid foodborne pathogen detection at attomolar level. *ACS Sensors*, *5*(5), 1427–1435. https://doi.org/10.1021/acssensors.0c00320

Wu, F., Zhao, S., Yu, B., Chen, Y. M., Wang, W., Song, Z. G., Hu, Y., Tao, Z. W., Tian, J. H., Pei, Y. Y., Yuan, M. L., Zhang, Y. L., Dai, F. H., Liu, Y., Wang, Q. M., Zheng, J. J., Xu, L., Holmes, E. C., & Zhang, Y. Z. (2020). A new coronavirus associated with human respiratory disease in China. *Nature*, *579*(7798), 265–269. https://doi.org/10.1038/s41586-020-2008-3

Xiang, Y., Lan, T., & Lu, Y. (2014). Using the widely available blood glucose meter to monitor insulin and HbA1c. *Journal of Diabetes Science and Technology (Online)*, *8*(4), 855–858. https://doi.org/10.1177/1932296814532875

Xiang, Y., & Lu, Y. (2011). Using personal glucose meters and functional DNA sensors to quantify a variety of analytical targets. *Nature Chemistry*, *3*(9), 697–703. https://doi.org/10.1038/nchem.1092

Xiang, Y., & Lu, Y. (2013). An invasive DNA approach toward a general method for portable quantification of metal ions using a personal glucose meter. *Chemical Communications*, *49*(6), 585–587. https://doi.org/10.1039/c2cc37156a

Xie, C., Jiang, L., Huang, G., Pu, H., Gong, B., Lin, H., Ma, S., Chen, X., Long, B., Si, G., Yu, H., Jiang, L., Yang, X., Shi, Y., & Yang, Z. (2020). Comparison of different samples for 2019 novel coronavirus detection by nucleic acid amplification tests. *International Journal of Infectious Diseases*, *93*, 264–267. https://doi.org/10.1016/j.ijid.2020.02.050

Xu, L., Dai, Q., Shi, Z., Liu, X., Gao, L., Wang, Z., Zhu, X., & Li, Z. (2020). Accurate MRSA identification through dual-functional aptamer and CRISPR-Cas12a assisted rolling circle amplification. *Journal of Microbiological Methods*, *173*, 105917. https://doi.org/10.1016/j.mimet.2020.105917

Yamano, T., Nishimasu, H., Zetsche, B., Hirano, H., Slaymaker, I. M., Li, Y., Fedorova, I., Nakane, T., Makarova, K. S., Koonin, E. V., Ishitani, R., Zhang, F., & Nureki, O. (2016). Crystal structure of Cpf1 in complex with guide RNA and target DNA. *Cell*, *165*(4), 949–962. https://doi.org/10.1016/j.cell.2016.04.003

Yan, C., Cui, J., Huang, L., Du, B., Chen, L., Xue, G., Li, S., Zhang, W., Zhao, L., Sun, Y., Yao, H., Li, N., Zhao, H., Feng, Y., Liu, S., Zhang, Q., Liu, D., & Yuan, J. (2020). Rapid and visual detection of 2019 novel coronavirus (SARS-CoV-2) by a reverse transcription loop-mediated isothermal amplification assay. *Clinical Microbiology and Infection*, *26*(6), 773–779. https://doi.org/10.1016/j.cmi.2020.04.001

Zhao, S., Lin, Q., Ran, J., Musa, S. S., Yang, G., Wang, W., Lou, Y., Gao, D., Yang, L., He, D., & Wang, M. H. (2020). Preliminary estimation of the basic reproduction number of novel coronavirus (2019-nCoV) in China, from 2019 to 2020: A data-driven analysis in the early phase of the outbreak. *International Journal of Infectious Diseases*, *92*, 214–217. https://doi.org/10.1016/j.ijid.2020.01.050

Zhou, P., Yang, X. L., Wang, X. G., Hu, B., Zhang, L., Zhang, W., Si, H. R., Zhu, Y., Li, B., Huang, C. L., Chen, H. D., Chen, J., Luo, Y., Guo, H., Jiang, R. D., Liu, M. Q., Chen, Y., Shen, X. R., Wang, X., … Shi, Z. L. (2020). A pneumonia outbreak associated with a new coronavirus of

probable bat origin. *Nature*, *579*(7798), 270–273. https://doi.org/10.1038/s41586-020-2012-7

Zhu, C. S., Liu, C. Y., Qiu, X. Y., Xie, S. S., Li, W. Y., Zhu, L., & Zhu, L. Y. (2020). Novel nucleic acid detection strategies based on CRISPR-Cas systems: From construction to application. *Biotechnology and Bioengineering*, *117*(7), 2279–2294. https://doi.org/10.1002/bit.27334

Zhu, N., Zhang, D., Wang, W., Li, X., Yang, B., Song, J., Zhao, X., Huang, B., Shi, W., Lu, R., Niu, P., Zhan, F., Ma, X., Wang, D., Xu, W., Wu, G., Gao, G. F., & Tan, W. (2020). A novel coronavirus from patients with pneumonia in china. *2019. N. Engl. J. Med. 382*(8), 727–733. https://doi.org/10.1056/NEJMoa2001017

SUPPORTING INFORMATION

Additional Supporting Information may be found online in the supporting information tab for this article.

How to cite this article: Huang D, Shi Z, Qian J, Bi K, Fang M, Xu Z. A CRISPR-Cas12a-derived biosensor enabling portable personal glucose meter readout for quantitative detection of SARS-CoV-2. *Biotechnology and Bioengineering*. 2021;118:1568–1577. https://doi.org/10.1002/bit.27673